Automotive Science and Engineering, Vol. 11, No. 2, (2021), 3569-3590

Iran University of Science and Technology

Automotive Science and Engineering

Journal Homepage: ase.iust.ac.ir

ISSN: 2717-2023

Improving the Lateral Stability of Road Vehicles Using Ladder Chassis Equipped with Linear Wave Springs

Mohammad. Shirzadifar[1*] ,Ali. Abdollahifar [2]

[1]Department of Mechanical Engineering, Yasouj University, Yasouj, Iran.

[2]Department of Mechanical Engineering, Shiraz University, Shiraz, Iran

ARTICLE INFO

Article history:

Received : 2 Dec 2020

Accepted: 26 May 2021

Published: 1 June 2021

Keywords:

Road vehicle

Ladder Frame

Linear Wave Spring

Vehicles Lateral Stability

Chassis FEM Analysis

A B S T R A C T

This paper introduces a new configuration of ladder chassis containing a set of linear wave springs to improve the lateral stability of road vehicles. The governing equations for lateral stability of the ladder frame equipped with linear wave springs were derived. In order to investigate this new system a unit base of the ladder frame equipped with linear wave springs and a typical ladder frame were modeled using FEM methods (ABAQUS) with the same size conditions. This comparative study is utilized to validate the derived equations and also to compare the effectiveness of the new designed system with typical ladder frames. Results indicate that the new system has considerably improved the lateral stability of the vehicle during road transportation and also noticeably decreased the stress on the side and cross members.

1. Introduction

Chassis in ground vehicles consisting of several types of frame structures is used to maintain all assembly units of the vehicle in the right order and withstand the longitudinal, lateral and vertical forces caused through transportation.

Chassis types can be classified by several characteristics such as: frame materials, number of wheels fitted in the vehicle, the number of driving wheels, the shape of the frame sections and the amount of integrity between the frame chassis and the vehicle's body. The ladder frame is the simplest and the oldest chassis design consisting of two symmetrical side members with an acceptable beam resistance.

The first use of ladder frame chassis goes back to the mid of the 1930's in race cars and cruciform bracing was added to them in order to increase the torsion stiffness.

In 1950's, Mercedes Benz and Auto Union modified the ladder frame chassis using different frame sections in three categories including channel section, box section and tabular section to overcome the lack of torsion stiffness. In early 1950s, Mercedes designers improved ladder frame chassis by mounting the cross members through the side members. Later, ladder frame chassis became less useful due to the lake of twin tube chassis efficiency as a result of the weight of the large tubes, although they had less priced production methodology.

Over recent decades, a number of investigations were conducted on different aspects of the vehicle's chassis:

- Dependence of truck roll stability on size and weight variables by Ervin in 1986 [1].

- Fatigue analysis of vehicular structure for VolvoS80 by Conle in 1997 [2].

- Evaluation of design alternatives for roll control of road vehicles by Cole in 2000 [3].

- Fundamentals of the lateral dynamics of road vehicles by Sharp in 2001[4].

*Mohammad Shirzadifar
Email Address: m.shirzadi1990@yahoo.com
http://dx.doi.org/10.22068/ase.2021.534

[Downloaded from www.iust.ac.ir on 2022-02-06]

[DOI: 10.22068/ase.2021.534]

- Normalized measure of relative roll instability for open-loop rollover warning by Kar and Rakheja in 2006 [5].

- Dynamics analysis of the cross member on a 4.5 ton truck chassis by Han Fui and Rahman in 2007 [6].

- Active chassis geometry for motorcycles by Šmiraus and Richtář in 2011[7].

- Standard stress analysis of truck chassis during ramping for evaluating frame strength by Asker1 and Salih in 2012 [8].

- Structural analysis of heavy vehicle chassis with different shapes of the cross sections by Sharma and colleagues in 2014 [9].

The successive studies in literature indicate that the frame designing methods are subject to continuous improvements, which leads to optimize common chassis structures to apply more payloads and stability for vehicles during road transportations. In recent years, a number of efforts had been made to improve the performance of vehicles by focusing on chassis performance via introducing new chassis structures, performing a number of simulation studies, suggesting new materials and patenting a number of chassis arrangements. Shin et al. presented new aluminum alloys for chassis [10] aiming at reducing the weight of the chassis, In another research, Autotech Engineering Deutschland GmbH invented new chassis link to improve the stiffness of chassis link [11], Ford Global Technologies, LLC, patented a chassis subframe arrangement to improve crash protection [12], Mazda Motor Corporation patented side chassis structure to absorb even a small vertical impact force applied to the side chassis structure[13] and ZF Friedrichshafen AG invented a chassis arrangement for utility vehicles [14]. Jonasson et al. at 2006 investigated an autonomous corner module as a facilitator for new vehicle chassis to increase vehicle's stability and handling [15]. A review on numerical analysis of vehicle chassis can be found in [16] suggesting ANSYS, ABAQUS and NASTRAN as the main FEA software to study chassis. To the best of our knowledge the modification of chassis structures involving a class of trucks hasn't been developed as ordinary urban vehicle's class, although their chassis torsional resistance has noticeable effects on truck's stability.

In order to develop the effects of truck's chassis on their lateral stability, this paper focuses on introducing new truck chassis structure containing ladder frame equipped with a set of linear wave springs to increase the lateral stability in road transportation.

Linear wave springs can serve as a lateral spring and is able to be located in the side members of the ladder frame owing to their particular shape. Wave springs were first developed by the USA SMALLEY industries in 1990's. Their stress equations are based on curved beams theories. They usually are categorized by their occupied area which is a function of their shapes (linear, circular or multiple structures) with four types of material. SMALLEY industries, mainly employe SAE 1070-1090 high carbon tempered spring steel, SAE1060-1075 high carbon cold drawn spring steel, and stainless steel 302 and 316 as these springs follow the hook's law [17].

The first idea of using wave springs in the vehicle's structure was attributed to Pavani and his research group in 2014. They analyzed wave springs to use them as an alternative for the helical compression springs in a vehicle's suspension [18]. In another research, Erfanian et al. evaluated the application of composite wave springs and the designing methods in chassis structure [19].

Although linear wave springs have been extensively used in different industries, still there is a lack of their application in vehicle's chassis structures to develop the stability.

The main purpose of this article is to design a new chassis structure based on using ordinary ladder frames and devising a set of linear wave springs inside the ladder chassis to increase the torsional resistance of the road vehicle's typical ladder frame and also to decrease the lateral forces such as cornering to improve road vehicle's lateral stability and tire's life cycle. The equations of lateral forces and main stresses of the ladder frame unit equipped with linear wave springs are calculated and then an application of using them for a road vehicle sample are modeled using FEM software (ABAQUS) to validate them and to evaluate their effects on improving lateral stability in comparison with an ordinary ladder frame unit with the same size order.

2. Introducing typical and multiple ladder frame chassis units consisting of linear wave springs

Typical ladder chassis includes several patterns of rectangular ladder frame units containing two side members and two cross members as shown in Figure1. The number of ladder frame unit patterns depends on the dimension of the vehicle's body, thus in order to determine the new structure of the

[Downloaded from www.iust.ac.ir on 2022-02-06]

[DOI: 10.22068/ase.2021.534]

ladder frame consists of wave springs, it is sufficient to introduce only one-unit base. The new proposed ladder frame unit has the main structure of ladder chassis equipped with two sets of linear wave springs inside each of the side members. As it is illustrated in Figure 2, each frame unit consists of two side members, two cross members, four sets of linear wave springs and two connecting planes. In order to supply enough space for wave springs and connecting plans inside the structure, the unit frame members should have boxing section (Figure 3). Each connecting plane is located between the middle inside place in the side members. The cross members are welded to the connecting plane with the same thickness as side member surfaces. The connecting planes are free to provide only lateral displacement along the lateral direction (Y direction in Figure 3). A set of linear wave spring is located in lateral direction between each side of the connecting plane and side members which has surface contact with each other.

enough space was prepared for them to have a deflection inside each side member along longitudinal direction (X direction in Figure 3) to release their energy. Therefore, the configuration of locating linear wave springs inside each of the side members do not have any effects on applied forces in longitudinal and vertical directions (X and Z directions in Figure 3). The member's dimension of the ladder frame unit equipped with linear wave springs is shown in Figure 4. So, the equipped ladder frame unit has only two connecting planes and four sets of linear wave springs in addition to the typical ladder frame unit which doesn't make much difference between frame unit's weights until they have the same size order. Based on Figures 1 and 4, the relations between the dimensions of the typical ladder frame unit and the one consists of linear wave springs should be as shown in Table 1 to be in the same size order.

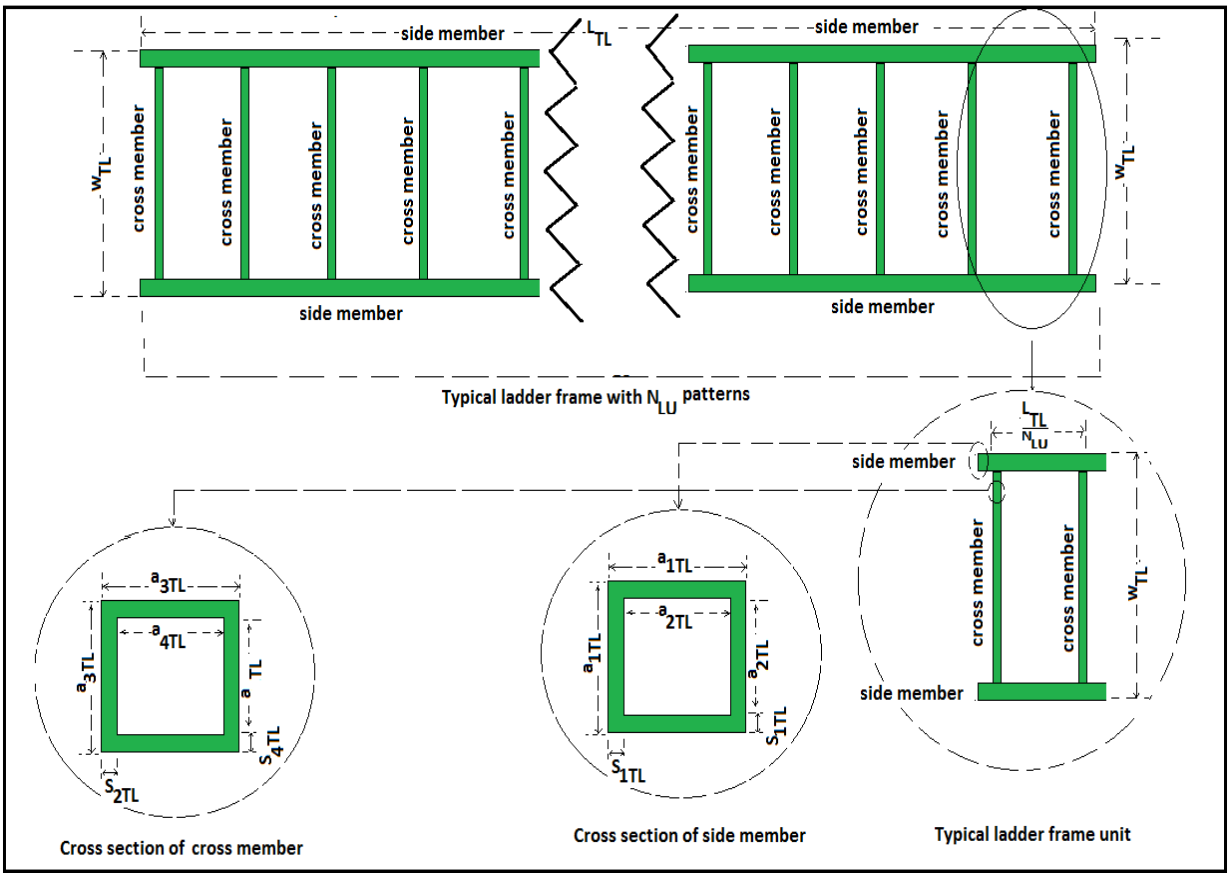

Figure 1: Schematic diagram of a typical ladder frame unit

The linear wave springs are activated when lateral forces are applied to the ladder frame unit along the lateral direction (Y direction in Figure 3) and

[Downloaded from www.iust.ac.ir on 2022-02-06]

[DOI: 10.22068/ase.2021.534]

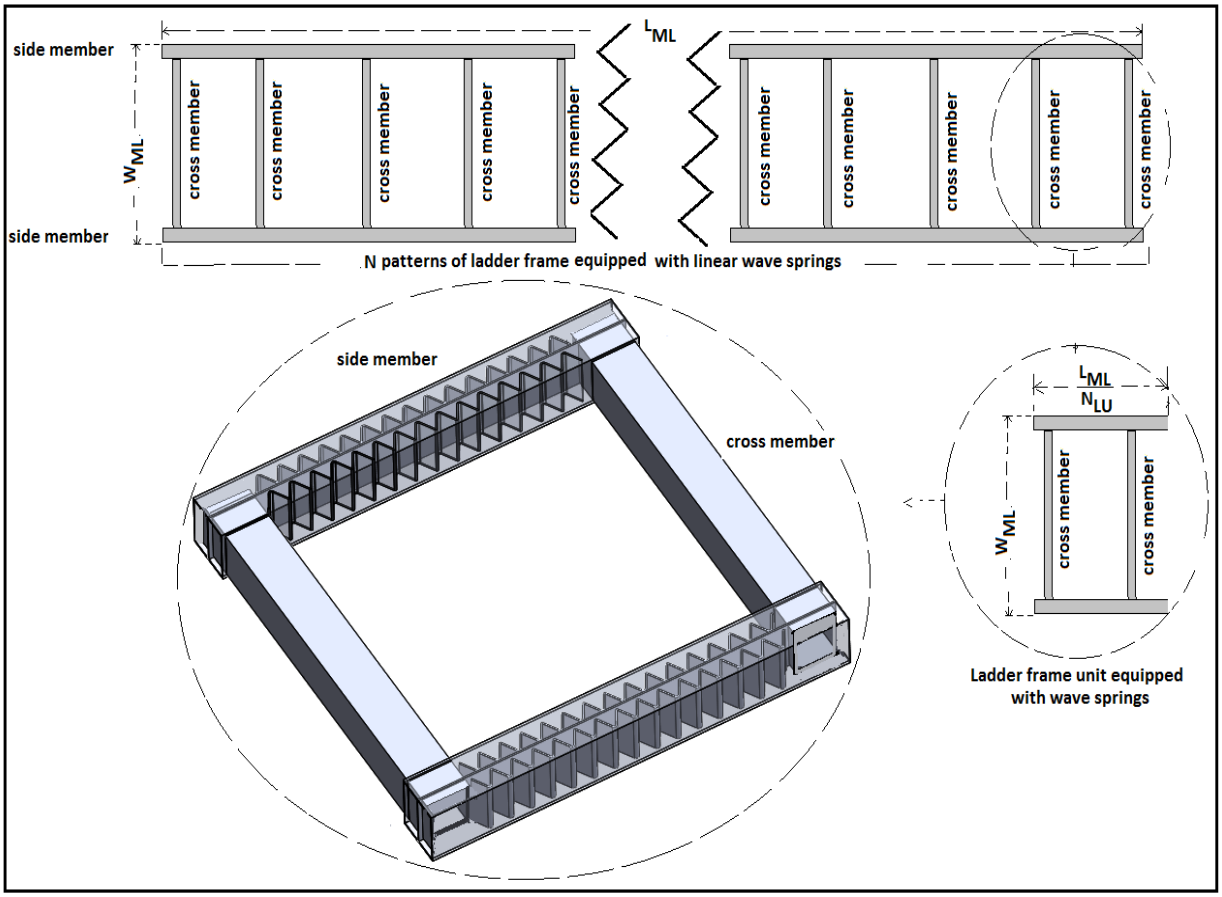

Figure 2: A ladder frame unit equipped with linear wave springs

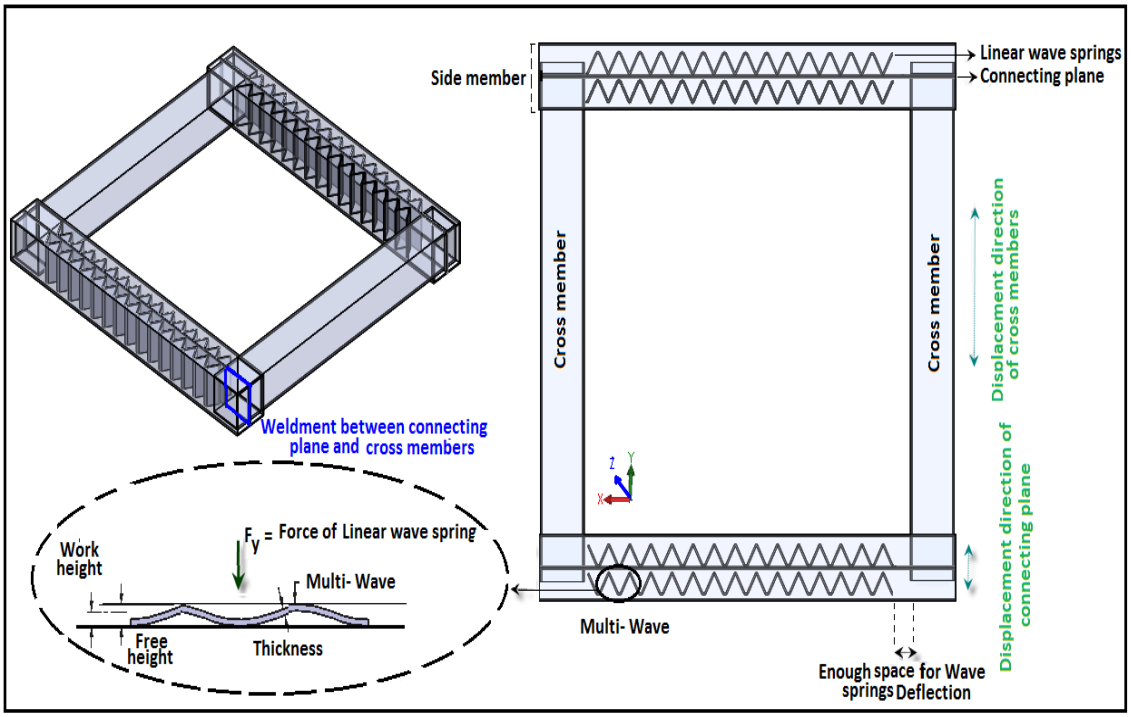

Figure 3: The structure of Ladder frame unit equipped with linear wave springs

[Downloaded from www.iust.ac.ir on 2022-02-06]

[DOI: 10.22068/ase.2021.534]

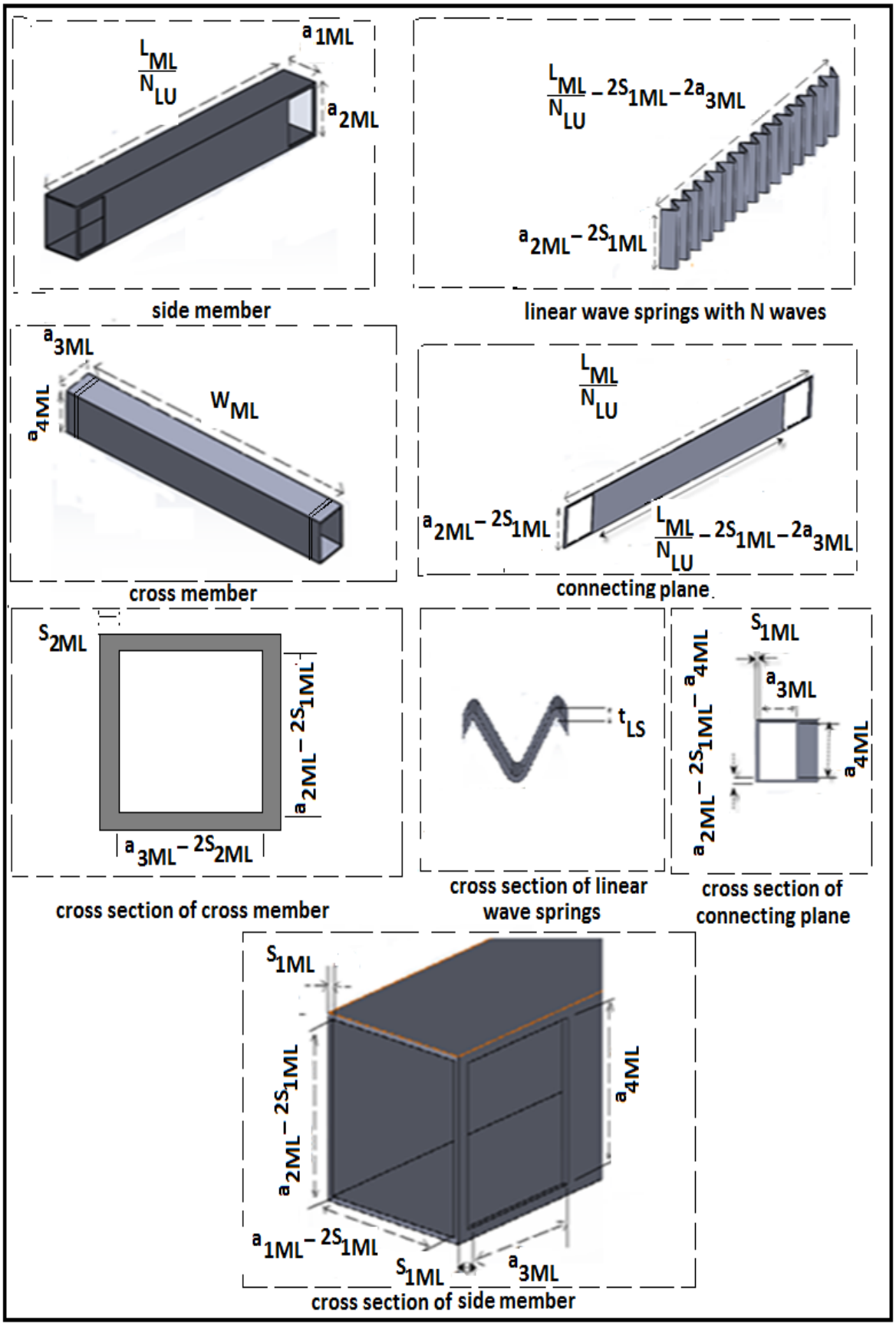

Figure 4: The member's dimension of the ladder frame unit equipped with wave springs

[Downloaded from www.iust.ac.ir on 2022-02-06]

[DOI: 10.22068/ase.2021.534]

Table 1: Dimensions relation between the typical ladder frame and the one consists of linear wave springs to be in the same size order

Parameters name	Parameters of frame for Fig. 1	Parameters of frame for Fig. 3	Relations between frames
Frame's longitudinal	L_{TL}	L_{ML}	$L_{TL} = L_{ML}$
Frame's width	W_{TL}	W_{ML}	$W_{TL} = W_{ML}$
Number of frame units	N_{LU}	N_{LU}	$N_{LU} = N_{LU}$
Longitudinal of side member's outer square cross section	a_{1TL}	a_{1ML}	$a_{1TL} = a_{1ML}$
Longitudinal of side member's inner square cross section	a_{2TL}	a_{2ML}	$a_{2TL} = a_{2ML}$
Thickness of side member's cross section	S_{1TL}	S_{1ML}	$S_{1TL} = S_{1ML}$
Longitudinal of cross member's outer square cross section	a_{3TL}	a_{3ML}	$a_{3TL} = a_{3ML}$
Longitudinal of cross member's inner square cross section	a_{4TL}	a_{4ML}	$a_{4TL} = a_{4ML}$
Thickness of cross member's cross section	S_{2TL}	S_{2ML}	$S_{2TL} = S_{2ML}$

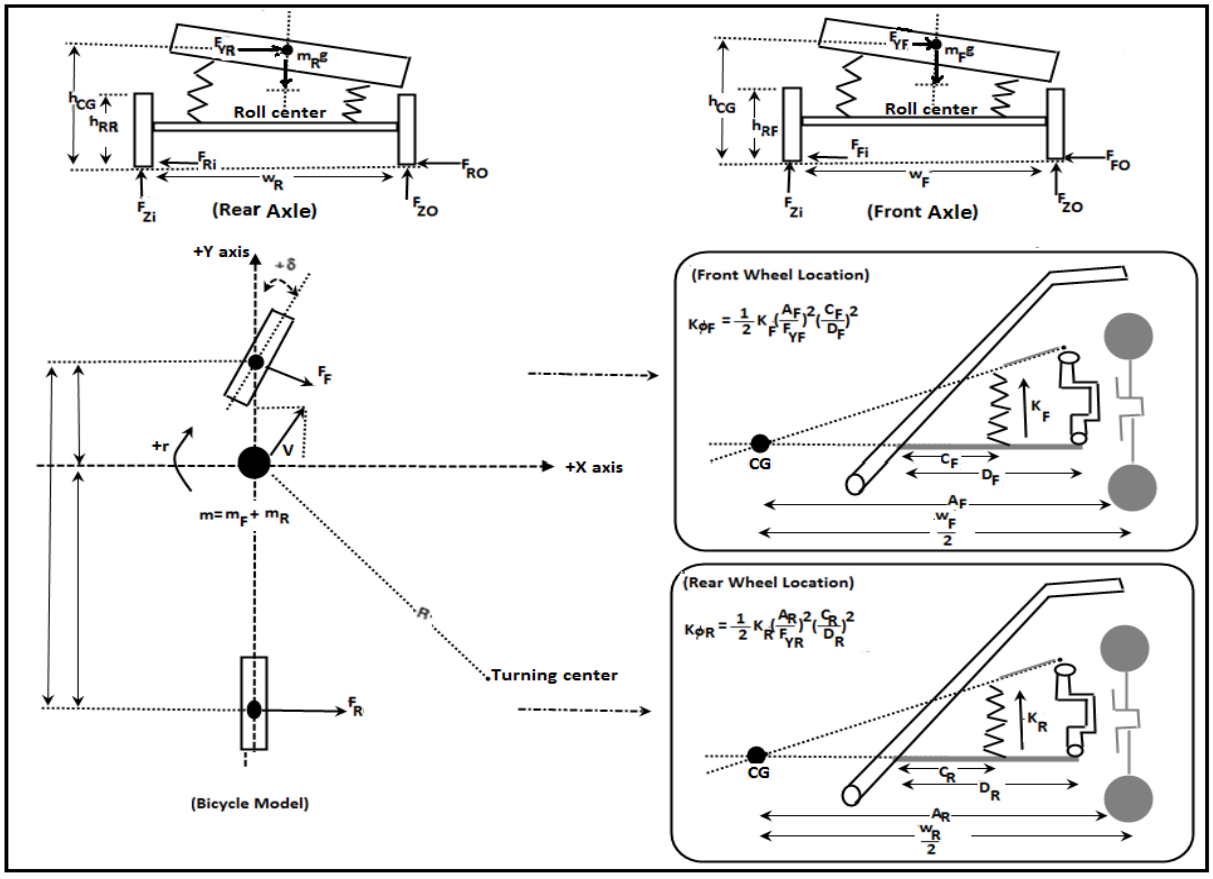

Figure 5: Elementary bicycle model of a vehicle

3. Methodology of evaluating frame unit

As mentioned before, the main purpose of introducing a new ladder frame unit equipped with linear wave springs is to reduce the destabilizing effects of vehicle's lateral forces applied to the chassis. In order to compare the lateral stability of the proposed ladder unit frame with the typical one, the vehicle's lateral forces stems from road transportation with direct effects on the frame unit of the chassis were calculated. Then the amount of frame unit lateral force which can be neutralized by linear wave springs was calculated based on the theory of linear wave springs. Finally, regarding the theory of stress-strain, the amount of net stress on each

[Downloaded from www.iust.ac.ir on 2022-02-06]

[DOI: 10.22068/ase.2021.534]

components of both ordinary and proposed ladder frame units caused by the net lateral force were calculated and compared together to investigate the improvement in the stability of the ladder frame unit equipped with linear wave springs.

4. Elementary vehicle analysis for calculating lateral forces on frame chassis

Lateral forces applied to vehicles during passing through a corner, includes three phases: the transient turn entry in which, vehicle's lateral velocity and turning moment increases from zero to their steady values; the steady state cornering that vehicle's lateral velocity and yawing moment remain constant with time and the vehicle is navigating a path with a cornering radius; the transient turn exit while vehicle's lateral velocity and moment return back to zero. Since calculating vehicle's lateral force is complex, a simple method named bicycle model was deployed. Regarding the bicycle theory as it is depicted in Figure 5, the lateral force applied on the chassis frames during vehicle's cornering can be calculated using equations 1 and 2 [20 -24]. Lateral force which is applied to the vehicle's chassis from the front wheels [20]:

$$F_{FO}+F_{Fi}=\frac{\varphi\left(k_{\varphi F}+k_{\varphi R}\right)}{m\,h_{CG}}\times \frac{m_F}{w_F}\times\left(\frac{h_{CG}k_{\varphi F}}{k_{\varphi F}+k_{\varphi R}}+\left(\frac{b}{L}h_{RF}\right)\right) \quad (1)$$

Lateral force which is applied to the vehicle's chassis from the rear wheels [20]:

$$F_{RO}+F_{Ri}=\frac{\varphi\left(k_{\varphi F}+k_{\varphi R}\right)}{m\,h_{CG}}\times \frac{m_R}{w_R}\times\left(\frac{h_{CG}k_{\varphi R}}{k_{\varphi F}+k_{\varphi R}}+\left(\frac{a}{L}h_{RR}\right)\right) \quad (2)$$

5. Elementary linear wave springs analysis for neutralizing frame chassis lateral force

Based on the installation position of linear wave springs in assemblies, the forces can act axially or radially.

In order to calculate deflection ($\triangle y_{LWS}$) and operating stress (S_{LWS}) of a linear wave spring with N waves, as it is shown in Figure 6, curved beam's theory and equations 3 and 4 were used [17]:

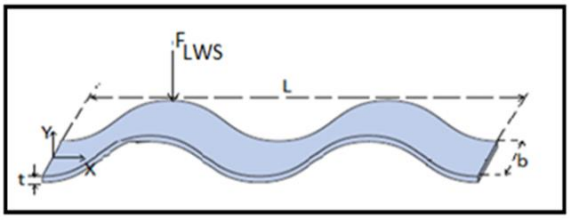

Figure 6: Linear wave spring dimensions with N waves and E modulus of elasticity

$$\triangle y_{LWS}=\frac{F_{LWS}L^3}{16\,E_{LWS}b\,t^3N^4} \quad (3)$$

$$S_{LWS}=\frac{3\,F_{LWS}L}{4\,b\,t^2N^2} \quad (4)$$

Therefore the linear spring stiffness (k_{LWS}) and its force (F_{LWS}) in linear wave spring, can be calculated by the equations (5) and (6) based on the hook's law.

$$k_{Lws}=\frac{16\,E_{LWS}b\,t^3N^4}{L^3} \quad (5)$$

$$F_{lws}=\frac{16\,E_{LWS}b\,t^3N^4}{L^3}\times\triangle y_{LWS} \quad (6)$$

Based on the dimensions that are used for each linear wave springs in Figure 7, the upper bound amounts of deflection for each of them in the frame assembly occurs when all of the waves are near to fade and the wave springs converts to a flat surface. Thus, the maximum deflection of each linear wave springs located inside of the side members in ladder frame unit can be determined as equation 7 based on reference [17].

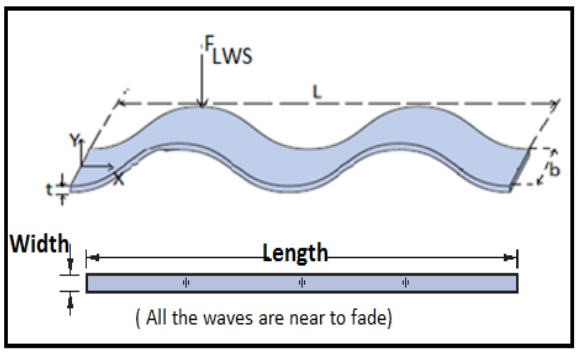

Figure 7: The shape of the linear wave springs when all of the waves are near to fade in the frame assembly

[Downloaded from www.iust.ac.ir on 2022-02-06]

[DOI: 10.22068/ase.2021.534]

(7)

$$\Delta y_{LWS}(max) = 0.02222\,N\times \left(\frac{\left(a_{1ML}-3S_{1ML}-2t_{LS}\right)^2+\frac{L^2}{N^2}}{8\left(a_{1ML}-3S_{1ML}-2t_{LS}\right)}\right)\times ARCsin\left(\frac{\frac{L}{N}\left(a_{1ML}-3S_{1ML}-2t_{LS}\right)}{\frac{\left(a_{1ML}-3S_{1ML}-2t_{LS}\right)^2}{4}+\frac{L^2}{4N^2}}\right)+t_{LS}$$

Now, by using the dimension's notation of the assembly showed in Figure 10 in equations (4), (5) and (6), the maximum amount of forces, operating stresses and spring stiffness created in each unit of linear wave spring can be calculated, respectively, by equations (A-1), (A-2) and (A-3) of the Appendix (A.1).

6. Calculating forces and stresses for both of the typical ladder frame units and the one equipped with wave springs

As it is shown in Figure 8, the typical ladder frame unit's free body diagram consists of front and rear lateral forces which results in a momentum (M_{TLS}) in the frame structure and makes the loss of vehicle's lateral stability under the effects of cornering. In regard with the Figures 1 and 8 and also equations (1) and (2), the amount of losing lateral stability of typical ladder frame unit's momentum under the effects of vehicle's cornering can be calculated from equation (8):

(8)

$$M_{TLS}=\frac{\varphi\ k_{\varphi F}+k_{\varphi R}}{N^2_{LU}mh_{CG}}\times\left[\left(\frac{am_F}{w_F}\times\left(\frac{h_{CG}k_{\varphi F}}{k_{\varphi F}+k_{\varphi R}}+\frac{b}{L_{TL}}h_{RF}\right)\right)-\left(\frac{bm_R}{w_R}\times\left(\frac{h_{CG}k_{\varphi R}}{k_{\varphi F}+k_{\varphi R}}+\frac{a}{L_{TL}}h_{RR}\right)\right)\right]$$

According to the effects of cornering on one typical ladder frame unit, Figure 1, equation (8) and by the help of reference [25], the critical states of stress for side and cross members are shown in Figure 9. Now based on the equation of normal stress (equation (9)) and Figure 9, the amount of maximum normal stresses of the side and cross members of the typical ladder frame unit can be calculated, respectively, by equations (10) and (11) as follows. According to the equation of normal stress from reference [25]:

(9)

$$\sigma_{max}=\frac{\sigma_X+\sigma_Y}{2}\pm\sqrt{\left(\frac{\sigma_X-\sigma_Y}{2}\right)^2+\tau^2_{XY}}\rightarrow$$

$$\sigma_{max}=\frac{0+\sigma_Y}{2}\pm\sqrt{\left(\frac{0-\sigma_Y}{2}\right)^2+0^2}\rightarrow\sigma_{max}=\sigma_Y$$

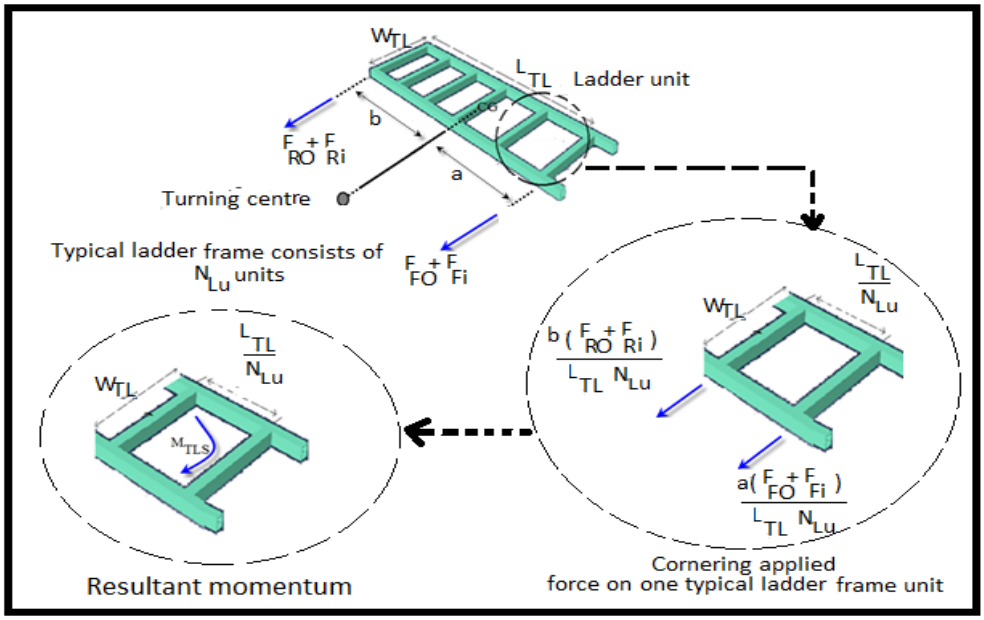

Figure 8: Free body diagrams for the typical ladder's frame under the effects of cornering

[Downloaded from www.iust.ac.ir on 2022-02-06]

[DOI: 10.22068/ase.2021.534]

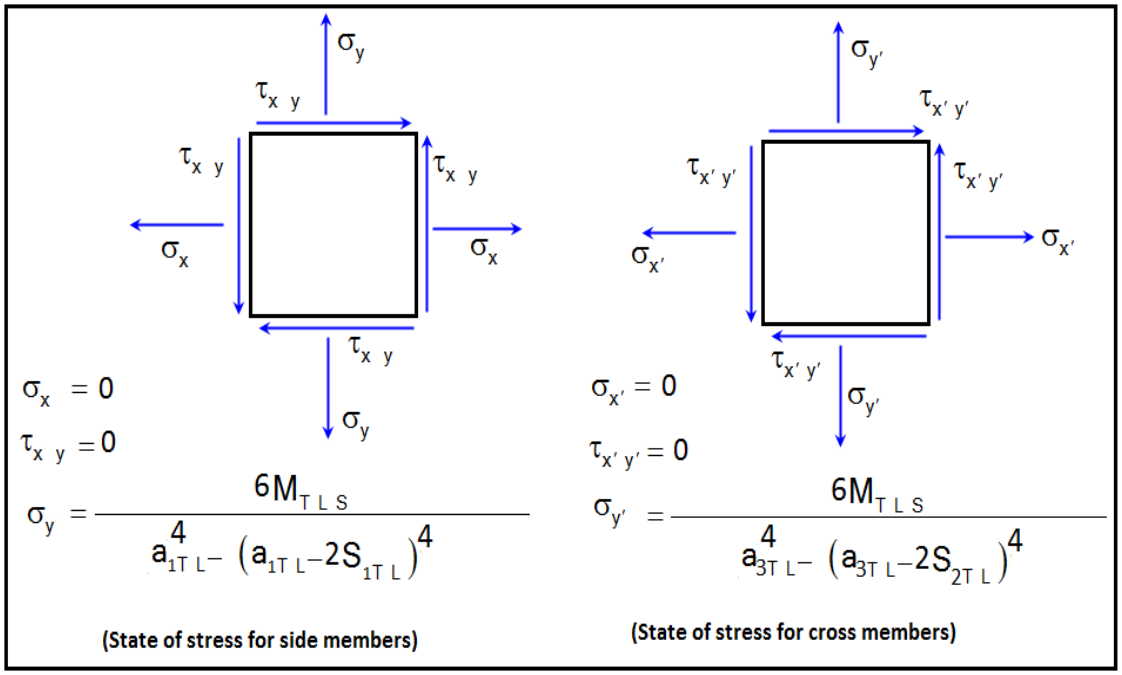

Figure 9: The critical states of stress for side and cross members of the typical ladder frame unit

According to the equations (8), (9) and Figure 9, maximum normal stress for the side member of the typical ladder frame unit (σ_{TLS}) equals:

(10)

$$\sigma_{TLS}=\frac{6\times\varphi\ k_{\varphi F}+k_{\varphi R}}{a_{1TL}^{\ 4}-a_{1TL}\text{-}2S_{1TL}^{\ \ 4}\times N^2_{LU}mh_{CG}}\times\left[\left(\frac{am_F}{w_F}\times\left(\frac{h_{CG}k_{\varphi F}}{k_{\varphi F}+k_{\varphi R}}+\frac{b}{L_{TL}}h_{RF}\right)\right)-\left(\frac{bm_R}{w_R}\times\left(\frac{h_{CG}k_{\varphi R}}{k_{\varphi F}+k_{\varphi R}}+\frac{a}{L_{TL}}h_{RR}\right)\right)\right]$$

According to the equations (8), (9) and Figure 9, maximum normal stress for the cross member of the typical ladder frame unit (σ_{TLC}) equals:

(11)

$$\sigma_{TLC}=\frac{6\times\varphi\ k_{\varphi F}+k_{\varphi R}}{a_{3TL}^{\ 4}-a_{3TL}\text{-}2S_{2TL}^{\ \ 4}\times N^2_{LU}mh_{CG}}\times\left[\left(\frac{am_F}{w_F}\times\left(\frac{h_{CG}k_{\varphi F}}{k_{\varphi F}+k_{\varphi R}}+\frac{b}{L_{TL}}h_{RF}\right)\right)-\left(\frac{bm_R}{w_R}\times\left(\frac{h_{CG}k_{\varphi R}}{k_{\varphi F}+k_{\varphi R}}+\frac{a}{L_{TL}}h_{RR}\right)\right)\right]$$

As it is shown in Figure 10, free body diagram of the ladder frame unit with linear wave springs under the effects of cornering consists of front and rear lateral forces that the a large portion of that can be neutralized by the action of wave springs. Thus, the amount of losing lateral stability (M_{MLS}), maximum normal stress for the side (σ_{MLS}) and cross members (σ_{MLC}) and the maximum normal stress for the connecting plane (σ_{MLP}) of the ladder frame unit consists of linear wave springs are respectively calculated by equations (A-4), (A-5), (A-6) and (A-7) of the Appendix (A.2).

[Downloaded from www.iust.ac.ir on 2022-02-06]

[DOI: 10.22068/ase.2021.534]

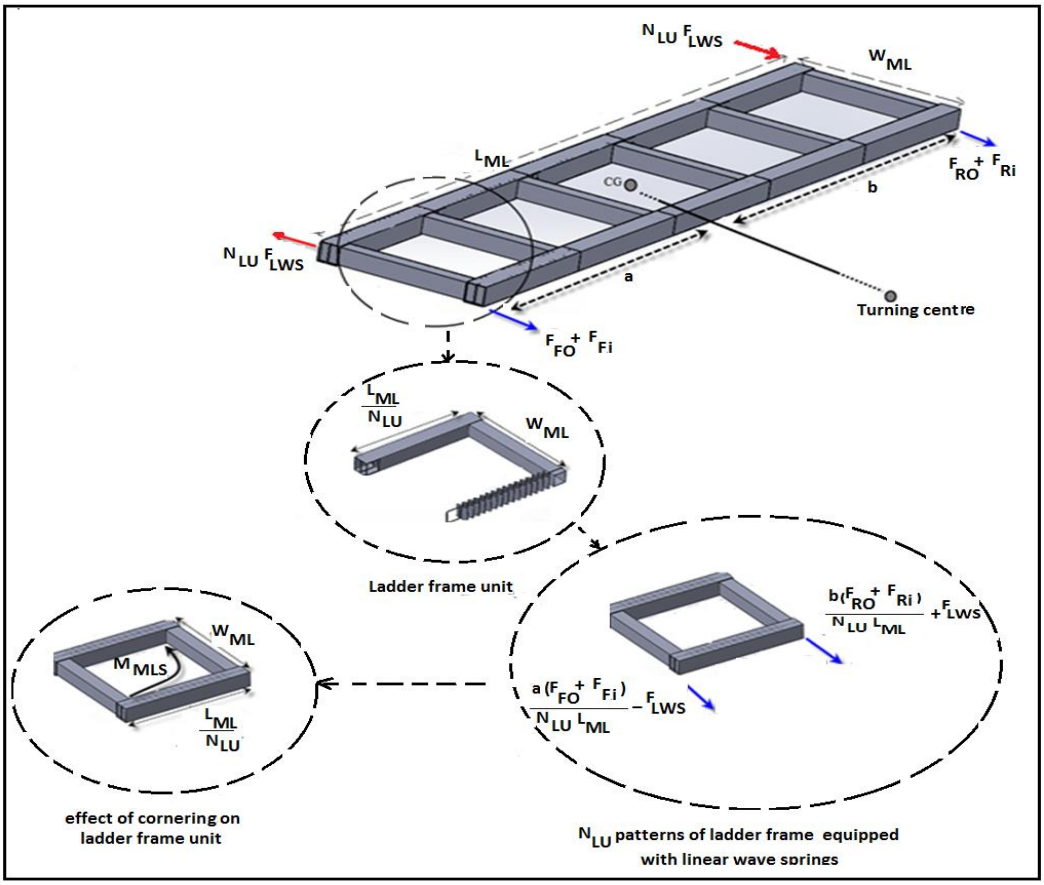

Figure 10: Free body diagrams for ladder frame equipped with linear wave springs under the effects of cornering

7. Comparison of the typical ladder frame unit and the one equipped with linear wave springs

Considering equations (8) and (A-4), the improvement of vehicle's lateral stability in proposed ladder frame unit can be calculated from equation (12):

$$\text{improving percent of Lateral stablity} = \frac{M_{TLS} - M_{MLS}}{M_{TLS}} \times 100 \quad (12)$$

Moreover, following equations (10) and (A-5), the reduction of normal stress for the side members in the frame unit with linear wave springs compared to the side members of the typical ladder frame unit, can be calculated as (13):

$$\text{decreasing percent of normal stress of side members frame unit} = \frac{\sigma_{TLS} - \sigma_{MLS}}{\sigma_{TLS}} \times 100 \quad (13)$$

Similarly, based on the equations (11) and (A-6), the normal stress reduction in the cross members of proposed frame was calculated using following equation (14):

$$\text{decreasing percent of normal stress of cross members frame unit} = \frac{\sigma_{TLC} - \sigma_{MLC}}{\sigma_{TLC}} \times 100 \quad (14)$$

8. Application of derived equations for ladder frame unit equipped with wave springs

Appendix (B) were selected as loading condition for two unit frames, including a typical and an equipped unit with linear wave spring with the same size order. Both unit frames modeled in FEM software (ABAQUS) with the boundary conditions and mesh settings as shown in Figure 11 and Table 2 under the static lateral loads of cornering. The stresses caused by lateral loads for the components of both unit frames calculated by the FEM software as indicated in Figure 12 for the typical frame unit and Figure 13 for the unit equipped with linear wave springs. In addition, stresses of both ladder frame units were calculated by the derived equations in Table 4 to make a comparison with the FEM software's results. According to Table 4 the discrepancies between the results of the calculated equations and FEM outputs was less than ten percent. These results, presented in Table 4, are a good proof to indicate the application of derived equations for both of the ladder frame units.

[Downloaded from www.iust.ac.ir on 2022-02-06]

[DOI: 10.22068/ase.2021.534]

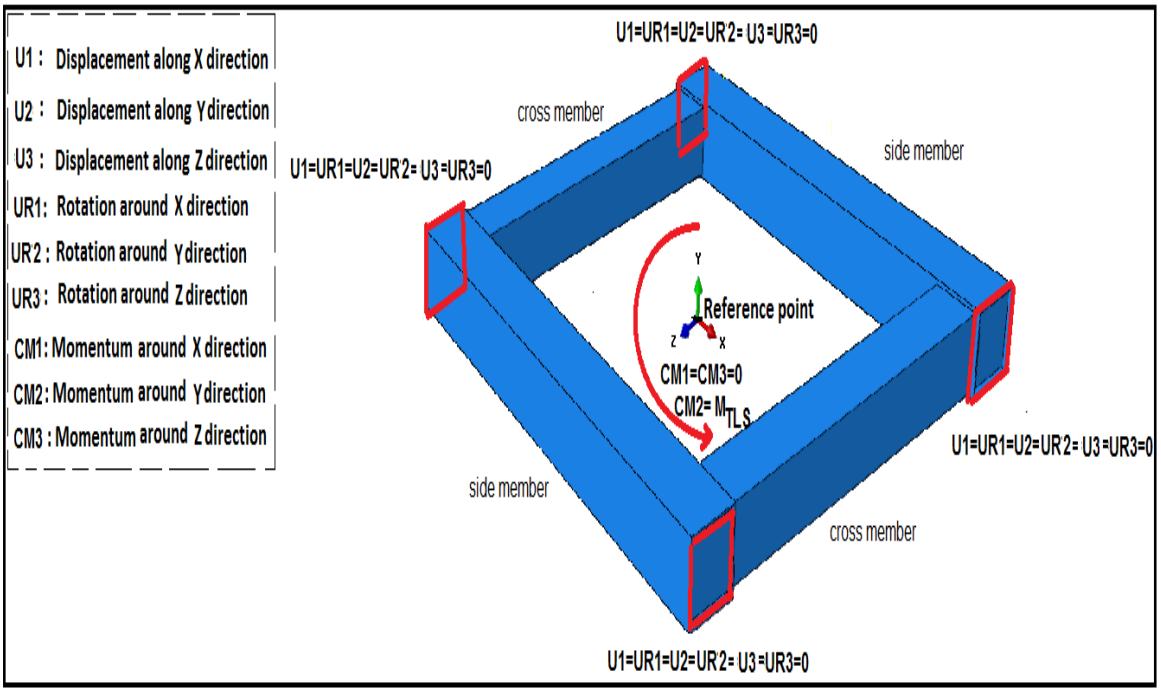

(a)

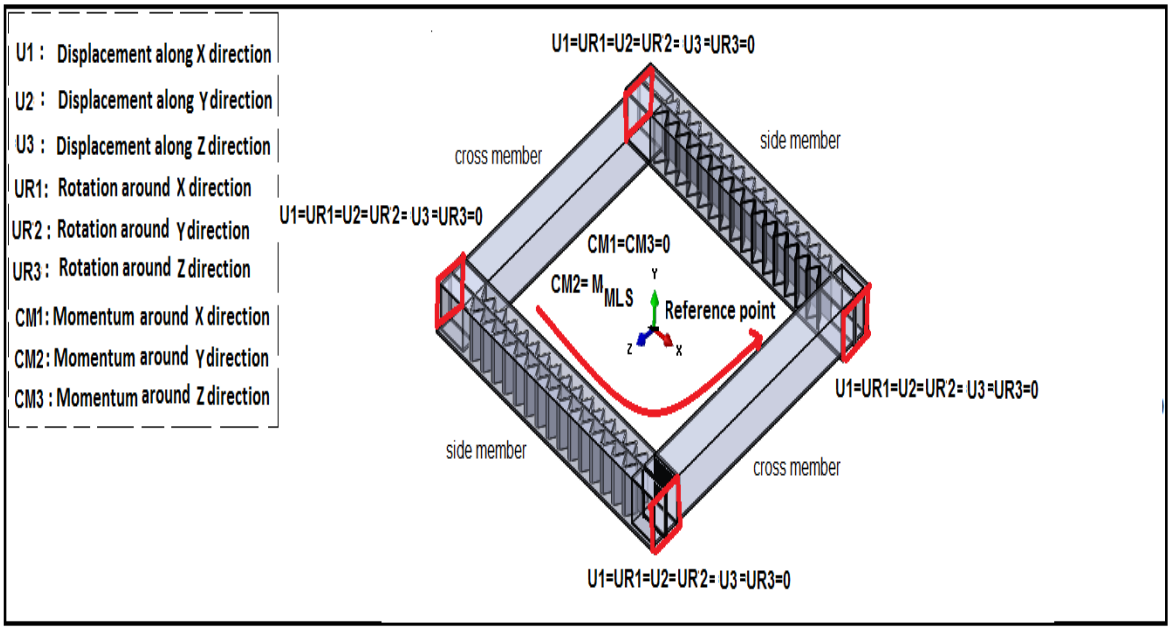

(b)

Figure 11: Boundary conditions in FEM software: a) For the typical ladder frame unit. b) For the ladder frame unit equipped with linear wave springs

[Downloaded from www.iust.ac.ir on 2022-02-06]

[DOI: 10.22068/ase.2021.534]

Table 2: Mesh settings for ladder frame units in FEM software

Mesh setting parameters	Mesh parameters for typical ladder frame unit	Mesh parameters for ladder frame unit equipped with linear wave springs
Number of nodes	15702	19603
Number of elements	9207	11039
Number of quadratic tetrahedral elements(C3D10)	4973	5614
Number of linear hexahedral elements(C3D8)	4234	5425
Average aspect ratio	1.08	1.11
Worst aspect ratio	2.03	2.27
Quad face comer angle less than 10 degrees	0%	0%
Quad face comer angle greater than 160 degrees	0%	0%

Table 3: Mesh study for ladder frame units analyzed by the FEM software

Number of elements for typical ladder frame unit	Max of normal stress for typical ladder frame unit	Convergence percent for typical ladder frame unit	Number of elements For ladder frame unit equipped with wave springs	Max of normal stress for ladder frame unit equipped with wave springs	Convergence percent for ladder frame unit equipped with wave springs
3151	38.11 Mpa	-	4392	1389.51 Mpa	-
5120	31.25 Mpa	18%	6268	1172.75 Mpa	15.6%
6324	26.47 Mpa	15.31%	7312	1009.15 Mpa	13.95%
7342	23.20 Mpa	12.36%	8536	876.95 Mpa	13.1%
8769	20.59 Mpa	11.24%	10031	769.61 Mpa	12.24%
9207	19.63 Mpa	4.68%	11039	744.6Mpa	3.25%

[Downloaded from www.iust.ac.ir on 2022-02-06]

[DOI: 10.22068/ase.2021.534]

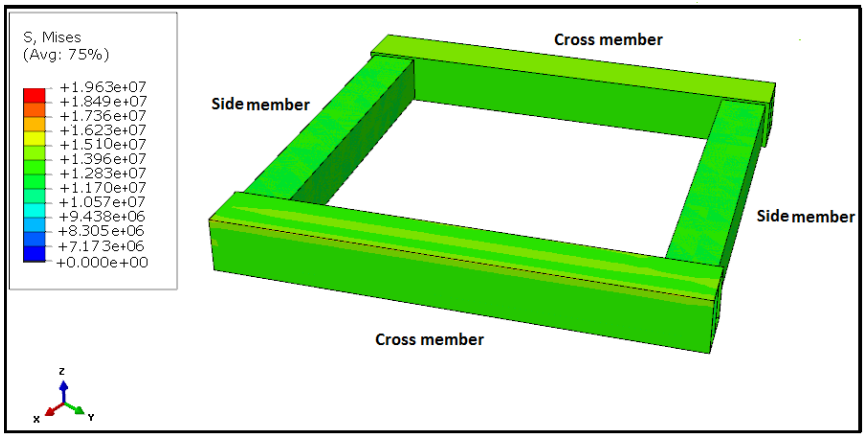

(a)

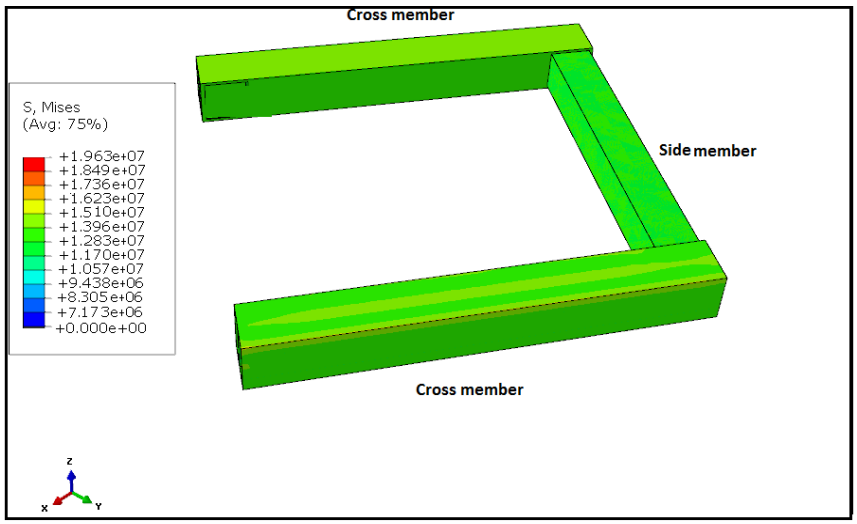

(b)

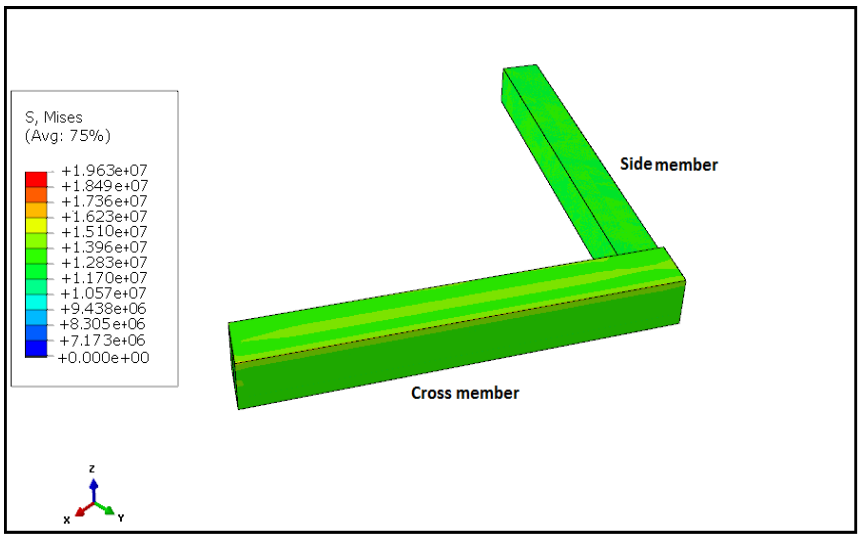

(c)

Figure 12: Stress contours analyzed by FEM software only under the effects of vehicle's cornering for: a) Typical ladder frame unit. b) Two cross member and one side member. c) Each side and cross member

[Downloaded from www.iust.ac.ir on 2022-02-06]

[DOI: 10.22068/ase.2021.534]

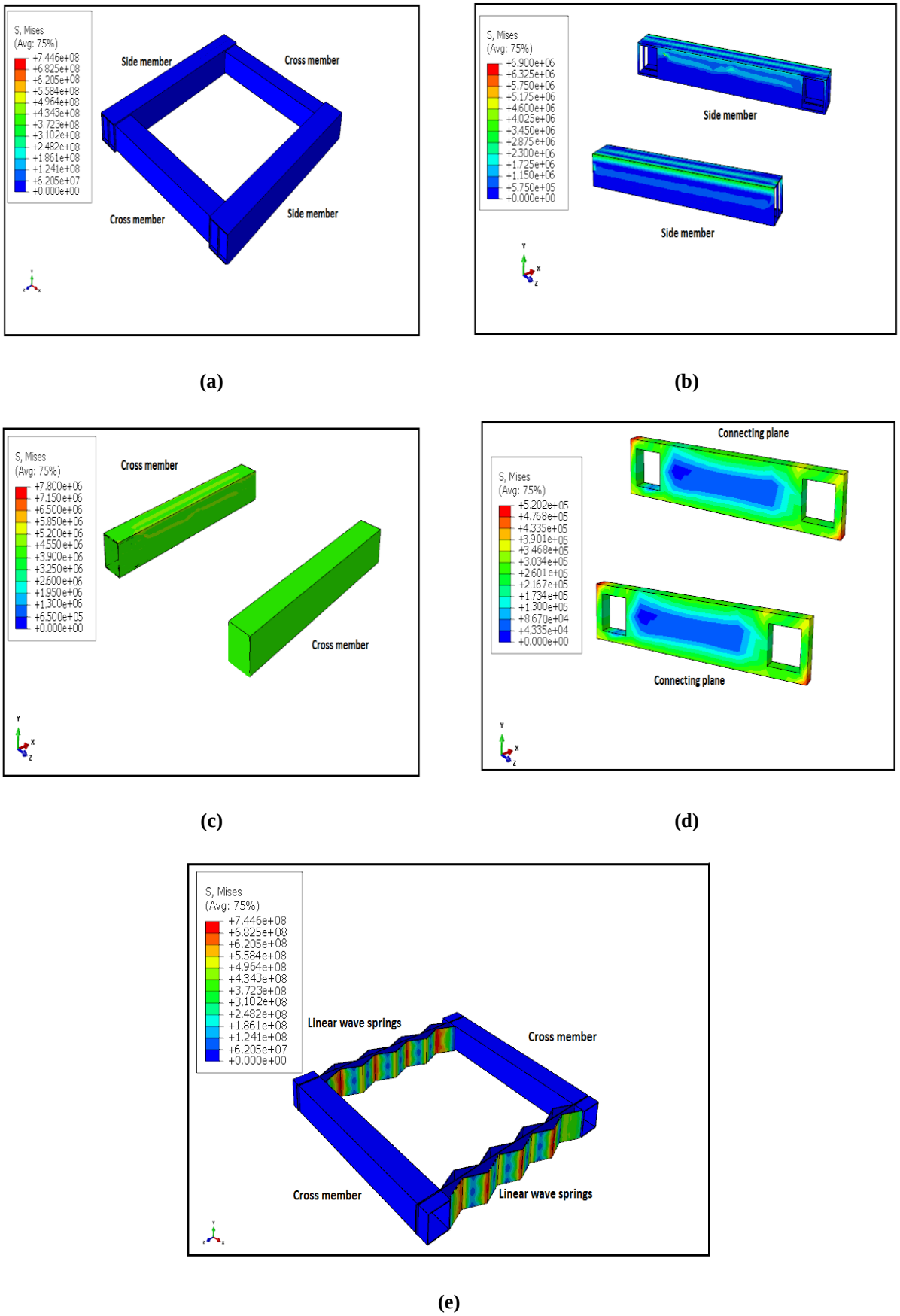

Figure 13: Stress contours of the ladder frame unit equipped with linear wave spring analyzed by FEM software only under the effects of vehicle's cornering for: a) Ladder frame unit. b) Side member. c) Cross member. d) Connecting plane. e) Linear wave springs

[Downloaded from www.iust.ac.ir on 2022-02-06]

[DOI: 10.22068/ase.2021.534]

Table 4: Stresses for the components of ladder frame units calculated by the gained equations and FEM software

Parameters	Calculated by equations for the typical ladder frame unit	Calculated by FEM software for the typical ladder frame unit	Calculated by equations for the ladder frame unit equipped with linear wave springs	Calculated by FEM software for the ladder frame unit equipped with linear wave springs
Normal stress of side members	15.37 Mpa	15.1 Mpa	6.54Mpa	6.9Mpa
Normal stress of cross members	17.82 Mpa	19.63Mpa	7.59Mpa	7.8Mpa
The normal stress of linear wave springs	-	-	738.82Mpa	744.6Mpa
The normal stress of connecting plane	-	-	0.49Mpa	0.52Mpa
The amount of momentum caused to lose lateral stability	-24.094kN.m	-	-10.26kN.m	-

9. Discussing the results

The introduced member's dimension of the equipped ladder frame unit in Figure 4 resulted in a 37.5 % of weights increase in comparison with the typical ladder frame unit since the connecting planes and wave springs have almost the same thickness and density as side member surfaces. Furthermore, as the locating configuration of linear wave spring inside the side members doesn't have any effects on the suspension's spring stiffness in vertical direction (Z direction in Figure 3), the vertical and longitudinal natural frequency of the new proposed ladder frame unit decreased for 16.5 % in comparison with the typical ladder frame unit only due to weights increasing. However, the linear wave springs inside the ladder frame units improving vehicle's lateral stability, decreasing normal stress on the unit frame's side and cross members are more than 57 percent, respectively, by equations (15), (16) and (17). This means, about 57 % of the energy caused by applying cornering force on the equipped ladder frame, absorbed by the linear wave springs deflection and its friction between the surface contact with the connecting plane and inner surface of the side members.

$$\text{improving percent of Lateral stablity} = \frac{(-24.094)-(-10.26)}{-24.094}\times 100 = 57.42\% \quad (15)$$

$$\text{decreasing percent of normal stress of side members frame unit} = \frac{(15.37)-(6.54)}{15.37}\times 100 = 57.45\% \quad (16)$$

$$\text{decreasing percent of normal stress of cross members frame unit} = \frac{(17.82)-(7.59)}{17.82}\times 100 = 57.41\% \quad (17)$$

10. CONCLUSION

In this paper, a new ladder frame chassis equipped with linear wave springs is introduced. As the configuration of locating wave springs inside the equipped frame only affects the lateral applied forces, only the governing equations of lateral frame's stability and normal stress on the components under the effects of vehicle's cornering forces were derived and compared with their counterparts in a typical ladder frame unit to indicate the advantages. In addition, the derived equations were validated considering a loading condition of a 10 ton truck chassis with 34 ton payload and using the analysis reports of the FEM software. The governing equations and FEM analysis compatibility indicated the effects of using linear wave springs in the ladder frame chassis on increasing lateral natural frequency**,** vehicle's lateral stability, decreasing the normal stress of the unit frame's cross and side members are more than 57 % and its inefficient effects on increasing weights, decreasing vertical and longitudinal natural frequency is less than 37.5 %. Linear wave springs were able to absorb 57 % of

[Downloaded from www.iust.ac.ir on 2022-02-06]

[DOI: 10.22068/ase.2021.534]

energy caused by applying cornering force on the equipped ladder frame and inefficient effects of locating them inside the structure of the ladder frame on increasing weights can be ignored in comparison with its advantages of increasing lateral natural frequency**,** vehicle's lateral stability, decreasing the normal stress of the unit frame's cross and side members. Furthermore, since the portion of the vehicle's lateral forces under the effect of cornering must be tolerated by the tires, decreasing the vehicle's lateral forces also can cause an increase tire's life cycle. Therefore, using ladder frame chassis equipped with linear wave springs can be more useful than typical ladder frame for road vehicles. Furthermore, to decrease the effects of locating linear wave springs inside the structure of ladder frame structure on increasing weights, it can be beneficial to study the effects of their replacement with the composite linear wave springs as the future work.

Declaration of Conflicting Interests

The authors confirm that the first author is with Yasouj University and the second author is with Shiraz University, and there is not any conflict of interest for this manuscript.

List of symbols

a	Longitudinal distance of C.G from vehicle's front
A_F	Lateral distance of front wheels from vehicle's central gravity
A_R	Lateral distance of rear wheels from vehicle's central gravity
a_{1TL} , a_{1ML}	Longitudinal of side member's outer square cross section
a_{2TL} , a_{2ML}	Longitudinal of side member's inner square cross section
a_{3TL} , a_{3ML}	Longitudinal of cross member's outer square cross section
b	Longitudinal distance of C.G from vehicle's rear
c_F	Lateral distance of front spring suspension from suspension 's link
c_R	Lateral distance of rear spring suspension from suspension 's link
D_F	Lateral distance of front wheel from suspension 's link
D_R	Lateral distance of rear wheel from suspension 's link
E	Modulus of Elasticity for side and cross members
E_{LWS}	Modulus of Elasticity for linear wave spring
F_{Zi} , F_{Zo}	Vertical force which is applied to each vehicle's wheels from road
F_{Fi} , F_{Fo}	Lateral force which is applied to vehicle's chassis from wheels
F_{LWS}	Force of linear wave spring applied to each frame unit
h_{CG}	Height of vehicle's central gravity
h_{RF}	Height of front roll centre
h_{RR}	Height of rear roll centre
k_F	Spring stiffness of front suspension
k_R	Spring stiffness of rear suspension
k_{LWS}	Spring stiffness of linear wave spring
$k_{\varphi F}$	Front roll stiffness of the suspension
$k_{\varphi R}$	Rear roll stiffness of the suspension
L_{TL} , L_{ML}	Frame's longitudinal
m	Vehicle's weight with its full load
m_F	Vehicle's front weight
m_R	Vehicle's rear weight
M_{MLS}	Momentum of ladder frame unit consists of wave springs
M_{TLS}	Momentum of typical ladder frame unit
N	Number of waves for each linear wave springs in frame unit
N_{LU}	Number of frame units
S_{LWS}	Operating stress of a linear wave springs with N waves
S_{1TL} , S_{1ML}	Thickness of side member's cross section
S_{2TL} , S_{2ML}	Thickness of cross member's cross section
t_{LS}	Thickness of linear wave spring
w_F	Front width of vehicle
w_R	Rear width of vehicle
w_{TL} , w_{ML}	Longitudinal of each cross members in frame unit
Δy_{LWS}	Deflection of a linear wave springs with N waves
ρ	Mass Density
δ	Ackermann steering angle
σ_{max}	Maximum principal stress
σ_{MLC}	Maximum normal stress of cross members in ladder frame unit contains wave springs
σ_{MLS}	Maximum normal stress of side members in ladder frame unit contains wave springs
σ_{TLC}	Maximum normal stress of cross members in typical ladder frame unit
σ_{MLP}	Maximum normal stress of connecting plane in ladder frame unit contains wave springs
σ_{TLS}	Maximum normal stress of side members in typical ladder frame unit
σ_T	Tensile Strength
σ_X , $\sigma_{X'}$, $\sigma_{X''}$	Normal stress of X direction
σ_Y, $\sigma_{Y'}$, $\sigma_{Y''}$	Normal stress of Y direction
σ_Y	Yield Strength
τ_{XY}, $\tau_{X'Y'}$, $\tau_{X''Y''}$	Shear stress in XY plane
φ	Rolling gradient

[Downloaded from www.iust.ac.ir on 2022-02-06]

[DOI: 10.22068/ase.2021.534]

References

[1] Ervin, R. D. "The dependence of truck roll stability on size and weight variables." International Journal of Vehicle Design 7.5-6 (1986): 192-208.

[2] Conle, F. A., and C-C. Chu. "Fatigue analysis and the local stress–strain approach in complex vehicular structures." International journal of fatigue 19.93 (1997): 317-323.

[3] Cole, D. J. "Evaluation of design alternatives for roll-control of road vehicles." Proceedings of the 5th International Symposium on Advanced Vehicle Control (AVEC 2000). University of Michigan, 2000.

[4] Sharp, Robin S. "Fundamentals of the lateral dynamics of road vehicles." Mechanics for a New Mellennium. Springer, Dordrecht, 2001. 127-146.

[5] Kar, Sandeep, Subhash Rakheja, and A. K. W. Ahmed. "A normalised measure of relative roll instability for open-loop rollover warning." International journal of heavy vehicle systems 13.1-2 (2006): 74-97.

[6] Fui, Teo Han, and Roslan Abd Rahman. "Statics and dynamics structural analysis of a 4.5 ton truck chassis." Jurnal Mekanikal 24.2 (2007).

[7] Šmiraus, Jakub, and Michal Richtář. "DESIGN OF MOTORCYLE ACTIVE CHASSIS GEOMETRY CHANGE SYSTEM."

[8] Asker, Haval Kamal, Thaker Salih Dawood, and Arkan Fawzi Said. "Stress analysis of standard truck chassis during Ramping on block using finite element method." ARPN Journal of Engineering and Applied Sciences 7.6 (2012): 641-648.

[9] Khan, Mohammad Mamoon. "Structural Analysis of a Heavy Vehicle Chassis Made of Different Alloys by Different Cross Sections." International Journal of Engineering Research 3.6 (2014).

[10] Shin, Jesik, et al. "Castability and mechanical properties of new 7xxx aluminum alloys for automotive chassis/body applications." Journal of Alloys and Compounds 698 (2017): 577-590.

[11] Haselhorst, Kai, Viktor Friesen, and Denis Geβner. "Chassis link for a motor vehicle." U.S. Patent No. 9,561,699. 7 Feb. 2017.

[12] Hilmann, Joergen, et al. "Chassis-subframe arrangement for improving crash protection." U.S. Patent No. 10,118,646. 6 Nov. 2018.

[13] NAKAUCHI, Shigeru, Nobuyuki Nakayama, and Takayuki Nakamae. "Side chassis structure of vehicle." U.S. Patent No. 10,173,731. 8 Jan. 2019.

[14] Langhorst, Friedhelm, et al. "Chassis system for a motor vehicle." U.S. Patent No. 10,214,068. 26 Feb. 2019.

[15] M. Jonasson, "Aspects of Autonomous Corner Modules as an Enabler for New Vehicle Chassis Solutions", Licentiate Thesis of Royal Institute of Technology Vehicle Dynamics, SE-100 44 Stockholm (ISSN 1651-7660), 2006.

[16] Vijayan, Singarajan Nagammal, and Sathiavelu Sendhilkumar. "Structural analysis of automotive chassis considering cross-section and material." International Journal of Mechanical Engineering and Automation 2.8 (2015): 370-376.

[17] Smalley production datasheets. Retrieved from https://www.smalley.com/sites/default /files/pdfs/Wave-Springs-CC2015: page 117.

[18] Pavani, P. N. L., et al. "Design, Modeling and Structural Analysis of Wave Springs." Procedia materials science 6 (2014): 988-995.

[19] Erfanian-Naziftoosi, H. R., Seyedmohammad S. Shams, and Rani Elhajjar. "Composite wave springs: Theory and design." Materials & Design 95 (2016): 48-53.

[20] Milliken, William F., and Douglas L. Milliken. "Race Car Vehicle Dynamics. Warrendale, PA: Society of Automotive Engineers." (1995).

[21] Smith, Carroll. Tune to win. Fallbrook: Aero Publishers, 1978.

[22] Beckman, Brian, and No Bucks Racing Club. "The physics of racing, part 5: Introduction to the racing line." online] http://www. esbconsult. com. au/ogden/locust/phors/phors05. htm (1991).

[23] Johnson, Charles Wayne. "Lateral stability of the driver/vehicle system: analytical results." (1983).

[24] Diaz, Alejandro. "FSAE 2015 Chassis and Suspension 25% Report." (2014): 71-79.

[25] Sadd, Martin H. Elasticity: theory, applications, and numerics. Academic Press, 2009: chapter2.

[Downloaded from www.iust.ac.ir on 2022-02-06]

[DOI: 10.22068/ase.2021.534]

Appendix A. Governing equations of linear wave springs

A.1. Calculating the maximum amount of forces, operating stresses and spring stiffness of linear wave springs

According to Figure (4), equations (6) and (7), the maximum forces of linear wave spring ($F_{lws}(\mathrm{max})$) can be calculated from equation (A-1).

(A-1)

$$F_{lws}(\mathrm{max})=\left(\frac{16E_{LWS}\times(a_{2ML}-2S_{1ML})\times t_{LS}^{3}N^{4}}{(\frac{L_{ML}}{N_{LU}}-2S_{1ML}-2a_{3ML})^{3}}\right)\times\left(0.02222N\times\left(\frac{(a_{1ML}-3S_{1ML}-2t_{LS})^{2}+\frac{\left(\frac{L_{ML}}{N_{LU}}-2S_{1ML}-2a_{3ML}\right)^{2}}{N^{2}}}{8\times(a_{1ML}-3S_{1ML}-2t_{LS})}\right)\times\mathrm{ARCsin}\left(\frac{\frac{\left(\frac{L_{ML}}{N_{LU}}-2S_{1ML}-2a_{3ML}\right)}{N}\times\frac{(a_{1ML}-3S_{1ML}-2t_{LS})}{\sqrt{\frac{(a_{1ML}-3S_{1ML}-2t_{LS})^{2}}{4}+\frac{\left(\frac{L_{ML}}{N_{LU}}-2S_{1ML}-2a_{3ML}\right)^{2}}{4N^{2}}}}}{}\right)+t_{LS}\right)$$

According to Figure (4), equations (4) and (A-1), the maximum operating stresses of linear wave springs ($S_{LWS}(\mathrm{max})$) can be calculated from equation (A-2).

(A-2)

$$S_{LWS}(\mathrm{max})=\frac{12E_{LWS}t_{LS}N^{2}}{(\frac{L_{ML}}{N_{LU}}-2S_{1ML}-2a_{3ML})^{2}}\times\left(\left(0.02222N\times\left(\frac{(a_{1ML}-3S_{1ML}-2t_{LS})^{2}+\frac{\left(\frac{L_{ML}}{N_{LU}}-2S_{1ML}-2a_{3ML}\right)^{2}}{N^{2}}}{8\times(a_{1ML}-3S_{1ML}-2t_{LS})}\right)\times\mathrm{ARCsin}\left(\frac{\frac{\left(\frac{L_{ML}}{N_{LU}}-2S_{1ML}-2a_{3ML}\right)}{N}\times\frac{(a_{1ML}-3S_{1ML}-2t_{LS})}{\sqrt{\frac{(a_{1ML}-3S_{1ML}-2t_{LS})^{2}}{4}+\frac{\left(\frac{L_{ML}}{N_{LU}}-2S_{1ML}-2a_{3ML}\right)^{2}}{4N^{2}}}}}{}\right)+t_{LS}\right)\right)$$

According to Figure (4) and equation (5), the maximum spring stiffness of linear wave springs (k_{Lws}) can be calculated from equation (A-3).

$$k_{Lws}=\frac{16E_{LWS}\times(a_{2ML}-2S_{1ML})\times t_{LS}^{3}N^{4}}{(\frac{L_{ML}}{N_{LU}}-2S_{1ML}-2a_{3ML})^{3}} \quad \text{(A-3)}$$

[Downloaded from www.iust.ac.ir on 2022-02-06]

[DOI: 10.22068/ase.2021.534]

A.2. Calculating the amount of losing lateral stability, maximum normal stress for the side and cross members and the maximum normal stress for the connecting plane of the ladder frame unit equipped with linear wave springs

According to Figures 4 and 9 and also equations (1), (2) and (A-1), the amount of losing lateral stability of the ladder frame unit equipped with linear wave springs under the effects of vehicle's cornering can be calculated from the frame unit's momentum (M_{MLS}) by equation (A-4). Based on Figures (4) and (10) and also equations (1), (2) and (A-1):

(A-4)

$$M_{MLS}=\left[\left(\frac{\varphi\,(k_{\varphi F}+k_{\varphi R})}{N^2_{LU}\, m\, h_{CG}}\times\left(\left(\frac{a\, m_F}{w_F}\times\left(\frac{h_{CG}k_{\varphi F}}{k_{\varphi F}+k_{\varphi R}}+\frac{b}{L_{ML}}h_{RF}\right)\right)-\left(\frac{b\, m_R}{w_R}\times\left(\frac{h_{CG}k_{\varphi R}}{k_{\varphi F}+k_{\varphi R}}+\frac{a}{L_{ML}}h_{RR}\right)\right)\right)\right)\right]-\left[\frac{L_{ML}}{N_{LU}}\times\left(\left(\frac{16\,E_{LWS}\times(a_{2ML}-2S_{1ML})\times t^3_{LS}N^4}{\left(\frac{L_{ML}}{N_{LU}}-2S_{1ML}-2a_{3ML}\right)^3}\right)\times\left(0.02222\,N\times\frac{(a_{1ML}-3S_{1ML}-2t_{LS})^2+\frac{\left(\frac{L_{ML}}{N_{LU}}-2S_{1ML}-2a_{3ML}\right)^2}{N^2}}{8\times(a_{1ML}-3S_{1ML}-2t_{LS})}\right)\; ARC\sin\left(\frac{\frac{\left(\frac{L_{ML}}{N_{LU}}-2S_{1ML}-2a_{3ML}\right)}{N}\times(a_{1ML}-3S_{1ML}-2t_{LS})}{\frac{(a_{1ML}-3S_{1ML}-2t_{LS})^2}{4}+\frac{\left(\frac{L_{ML}}{N_{LU}}-2S_{1ML}-2a_{3ML}\right)^2}{4N^2}}\right)+t_{LS}\right)\right]$$

According to the effects of cornering on ladder frame unit equipped with linear wave springs, Figure 4, equation (A-4) and by the help of reference [25], the critical states of stress for side and cross members and also the connecting plane are as shown in Figure (A-1).

Now, based on the equation of normal stress (equation (9)) and Figure (A-1), the amount of maximum normal stresses of side and cross members and also the connecting plane of the ladder frame unit consists of linear wave springs can be calculated by equations (A-5), (A-6) and (A-7) as below, respectively. According to the equations (9) and (A-4) and Figure (A-1), maximum normal stress for the side member of the ladder frame unit equipped with linear wave springs (σ_{MLS}) equals:

(A-5)

$$\sigma_{MLS}=\frac{6}{a^4_{1ML}-(a_{1ML}-2S_{1ML})^4}\times\left[\left[\frac{\varphi\,(k_{\varphi F}+k_{\varphi R})}{N^2_{LU}\, m\, h_{CG}}\times\left(\left(\frac{a\, m_F}{w_F}\times\left(\frac{h_{CG}k_{\varphi F}}{k_{\varphi F}+k_{\varphi R}}+\frac{b}{L_{ML}}h_{RF}\right)\right)-\left(\frac{b\, m_R}{w_R}\times\left(\frac{h_{CG}k_{\varphi R}}{k_{\varphi F}+k_{\varphi R}}+\frac{a}{L_{ML}}h_{RR}\right)\right)\right)\right]-\left[\frac{L_{ML}}{N_{LU}}\times\left(\left(\frac{16\,E_{LWS}\times(a_{2ML}-2S_{1ML})\times t^3_{LS}N^4}{\left(\frac{L_{ML}}{N_{LU}}-2S_{1ML}-2a_{3ML}\right)^3}\right)\times\left(0.02222\,N\times\frac{(a_{1ML}-3S_{1ML}-2t_{LS})^2+\frac{\left(\frac{L_{ML}}{N_{LU}}-2S_{1ML}-2a_{3ML}\right)^2}{N^2}}{8\times(a_{1ML}-3S_{1ML}-2t_{LS})}\right)\; ARC\sin\left(\frac{\frac{\left(\frac{L_{ML}}{N_{LU}}-2S_{1ML}-2a_{3ML}\right)}{N}\times(a_{1ML}-3S_{1ML}-2t_{LS})}{\frac{(a_{1ML}-3S_{1ML}-2t_{LS})^2}{4}+\frac{\left(\frac{L_{ML}}{N_{LU}}-2S_{1ML}-2a_{3ML}\right)^2}{4N^2}}\right)+t_{LS}\right)\right]\right]$$

[DOI: 10.22068/ase.2021.534]
[Downloaded from www.iust.ac.ir on 2022-02-06]

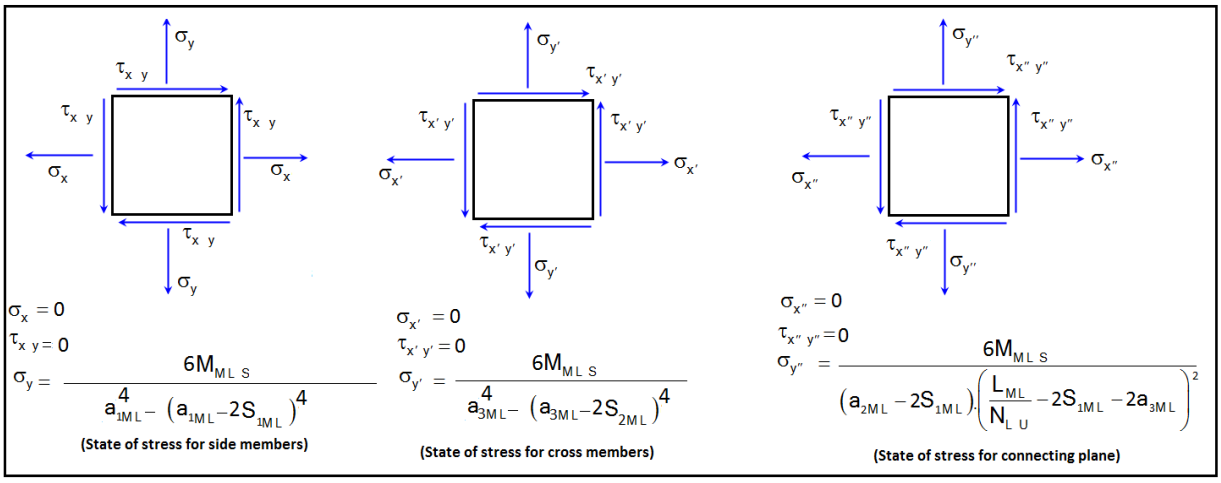

Figure A-1: Critical states of stress for the side and cross members of the ladder frame unit equipped with linear wave springs.

According to the equations (9) and (A-4) and Figure (A-1), the maximum normal stress of the cross member of ladder frame unit equipped with linear wave springs (σ_{MLC}) calculated from equation (A-6) and also According to the equations (9) and (A-4) and Figure (A-1), the maximum normal stress on the connecting plane of the ladder frame unit equipped with linear wave springs calculated from equation (A-7).

[Downloaded from www.iust.ac.ir on 2022-02-06]

[DOI: 10.22068/ase.2021.534]

(A-6)

$$\sigma_{MLc}=\frac{6}{a_{3ML}^{4}-a_{3ML}-2S_{2ML}}\times\left[\left[\left(\frac{\varphi\,k_{\varphi F}+k_{\varphi R}}{N_{LU}^{2}m\,h_{CG}}\times\left(\left(\frac{a\,m_F}{w_F}\times\left(\frac{h_{CG}k_{\varphi F}}{k_{\varphi F}+k_{\varphi R}}+\frac{b}{L_{ML}}h_{RF}\right)\right)-\left(\frac{b\,m_R}{w_R}\times\left(\frac{h_{CG}k_{\varphi R}}{k_{\varphi F}+k_{\varphi R}}+\frac{a}{L_{ML}}h_{RR}\right)\right)\right)\right)\right]-\left[\left(\frac{16E_{LWS}\times(a_{2ML}-2S_{1ML})\times t_{LS}^{3}N^{4}}{\left(\frac{L_{ML}}{N_{LU}}-2S_{1ML}-2a_{3ML}\right)^{3}}\right)\times\left[\frac{L_{ML}}{N_{LU}}\times\left[\left(0.02222N\times\frac{(a_{1ML}-3S_{1ML}-2t_{LS})^{2}+\frac{\left(\frac{L_{ML}}{N_{LU}}-2S_{1ML}-2a_{3ML}\right)^{2}}{N^{2}}}{8\times(a_{1ML}-3S_{1ML}-2t_{LS})}\right)\right.\right.\right.\left.\left.\left.ARCsin\left(\frac{\frac{\left(\frac{L_{ML}}{N_{LU}}-2S_{1ML}-2a_{3ML}\right)}{N}\times\frac{(a_{1ML}-3S_{1ML}-2t_{LS})}{(a_{1ML}-3S_{1ML}-2t_{LS})^{2}+\frac{\left(\frac{L_{ML}}{N_{LU}}-2S_{1ML}-2a_{3ML}\right)^{2}}{4N^{2}}}\right)+t_{LS}\right)\right]\right]\right]$$

(A-7)

$$\sigma_{MLP}=\frac{6}{a_{2ML}-2S_{1ML}\times\left(\frac{L_{ML}}{N_{LU}}-2S_{1ML}-2a_{3ML}\right)^{2}}\times\left[\left[\left(\frac{\varphi\,k_{\varphi F}+k_{\varphi R}}{N_{LU}^{2}m\,h_{CG}}\times\left(\left(\frac{a\,m_F}{w_F}\times\left(\frac{h_{CG}k_{\varphi F}}{k_{\varphi F}+k_{\varphi R}}+\frac{b}{L_{ML}}h_{RF}\right)\right)-\left(\frac{b\,m_R}{w_R}\times\left(\frac{h_{CG}k_{\varphi R}}{k_{\varphi F}+k_{\varphi R}}+\frac{a}{L_{ML}}h_{RR}\right)\right)\right)\right)\right]-\left[\left(\frac{16E_{LWS}\times(a_{2ML}-2S_{1ML})\times t_{LS}^{3}N^{4}}{\left(\frac{L_{ML}}{N_{LU}}-2S_{1ML}-2a_{3ML}\right)^{3}}\right)\times\left[\frac{L_{ML}}{N_{LU}}\times\left[\left(0.02222N\times\frac{(a_{1ML}-3S_{1ML}-2t_{LS})^{2}+\frac{\left(\frac{L_{ML}}{N_{LU}}-2S_{1ML}-2a_{3ML}\right)^{2}}{N^{2}}}{8\times(a_{1ML}-3S_{1ML}-2t_{LS})}\right)\right.\right.\right.\left.\left.\left.ARCsin\left(\frac{\frac{\left(\frac{L_{ML}}{N_{LU}}-2S_{1ML}-2a_{3ML}\right)}{N}\times\frac{(a_{1ML}-3S_{1ML}-2t_{LS})}{(a_{1ML}-3S_{1ML}-2t_{LS})^{2}+\frac{\left(\frac{L_{ML}}{N_{LU}}-2S_{1ML}-2a_{3ML}\right)^{2}}{4N^{2}}}\right)+t_{LS}\right)\right]\right]\right]$$

Appendix B. Characteristics of the case study

B.1. Introducing the characteristics of the truck chassis used for the study

The characteristics of the truck chassis used as an application of the calculated equations are introduced in Table (B-1).

[Downloaded from www.iust.ac.ir on 2022-02-06]

[DOI: 10.22068/ase.2021.534]

Table B-1: Characteristics of the truck chassis used for the study

Parameters symbol	Parameters amount for typical unit	Parameters amount for unit consists of linear wave springs
-	AISI 4130 alloy	AISI 4130 alloy
-	0.30 C, 1.0 Cr, 0.90 Mn, 0.20 Mo	0.30 C, 1.0 Cr, 0.90 Mn, 0.20 Mo
E	207 GPa	207 GPa
ρ	$7798\frac{kg}{m^3}$	$7798\frac{kg}{m^3}$
σ_Y	910 Mpa	910 Mpa
σ_T	1030 Mpa	1030 Mpa
φ	0.5 rad	0.5 rad
$k_{\varphi F}$	$375\frac{kN}{m}$	$375\frac{kN}{m}$
$k_{\varphi R}$	$1025\frac{kN}{m}$	$1025\frac{kN}{m}$
m	44000 kg	44000 kg
h_{CG}	2.1 m	2.1m
N_{LU}	5	5
L_{TL} , L_{ML}	7.8 m	7.8 m
a	4.9m	4.9m
b	2.9m	2.9m
h_{RF}	1.1m	1.1m
h_{RR}	1.1m	1.1m
w_F	2.04m	2.04m
w_R	1.82m	1.82m
m_F	13040kg	13040kg
m_R	30960kg	30960kg
a_{1TL} , a_{1ML}	0.29m	0.29m
a_{2TL} , a_{2ML}	0.27m	0.27m
S_{1TL} , S_{1ML}	0.01m	0.01m
a_{3TL} , a_{3ML}	0.27m	0.27m
a_{4TL} , a_{4ML}	0.25m	0.25m
S_{2TL} , S_{2ML}	0.01m	0.01m
t_{LS}	-	0.01m
N	-	4
$\frac{L_{TL}}{N_{LU}}$, $\frac{L_{ML}}{N_{LU}}$	1.56m	1.56m
w_{TL} , w_{ML}	0.60m	0.60m
E_{LWS}	203.4 Gpa	203.4 Gpa
$\frac{L_{ML}}{N_{LU}} - 2\,S_{1ML} - 2\,a_{3ML}$	-	1m
$a_{2ML} - 2\,S_{1ML}$	-	0.25m
$\frac{L_{ML}}{N_{LU}}$	-	1.56m
$a_{2ML} - 2\,S_{1ML}$	-	0.25m
S_{1ML}	-	0.01m

[Downloaded from www.iust.ac.ir on 2022-02-06]

[DOI: 10.22068/ase.2021.534]